Filling gaps in the soundscape of gravitational waves

Diego Blas

based on 2107.04063/2107.04601

w. Alex Jenkins

Universitat Autònoma de Barcelona

IFAE BIST Barcelona Institute of Science and Technology

Ayuda Beatriz Galindo Senior
BG20/00228

GOBIERNO DE ESPAÑA MINISTERIO DE UNIVERSIDADES

MINISTERIO DE CIENCIA E INNOVACIÓN

AGENCIA ESTATAL DE INVESTIGACIÓN

MW in visible band

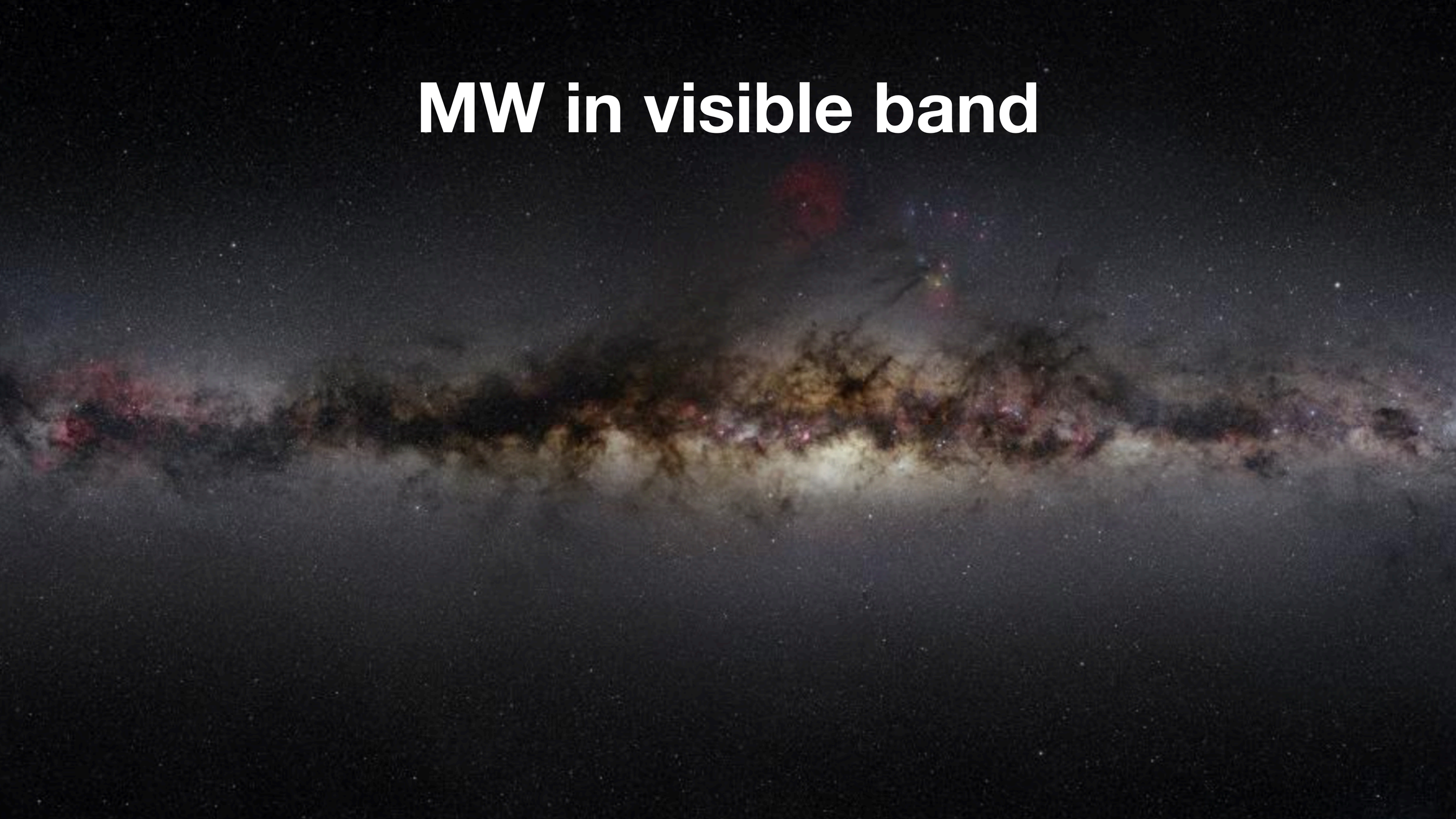

MW in radio band

Stochastic gravitational-wave background (SGWB)

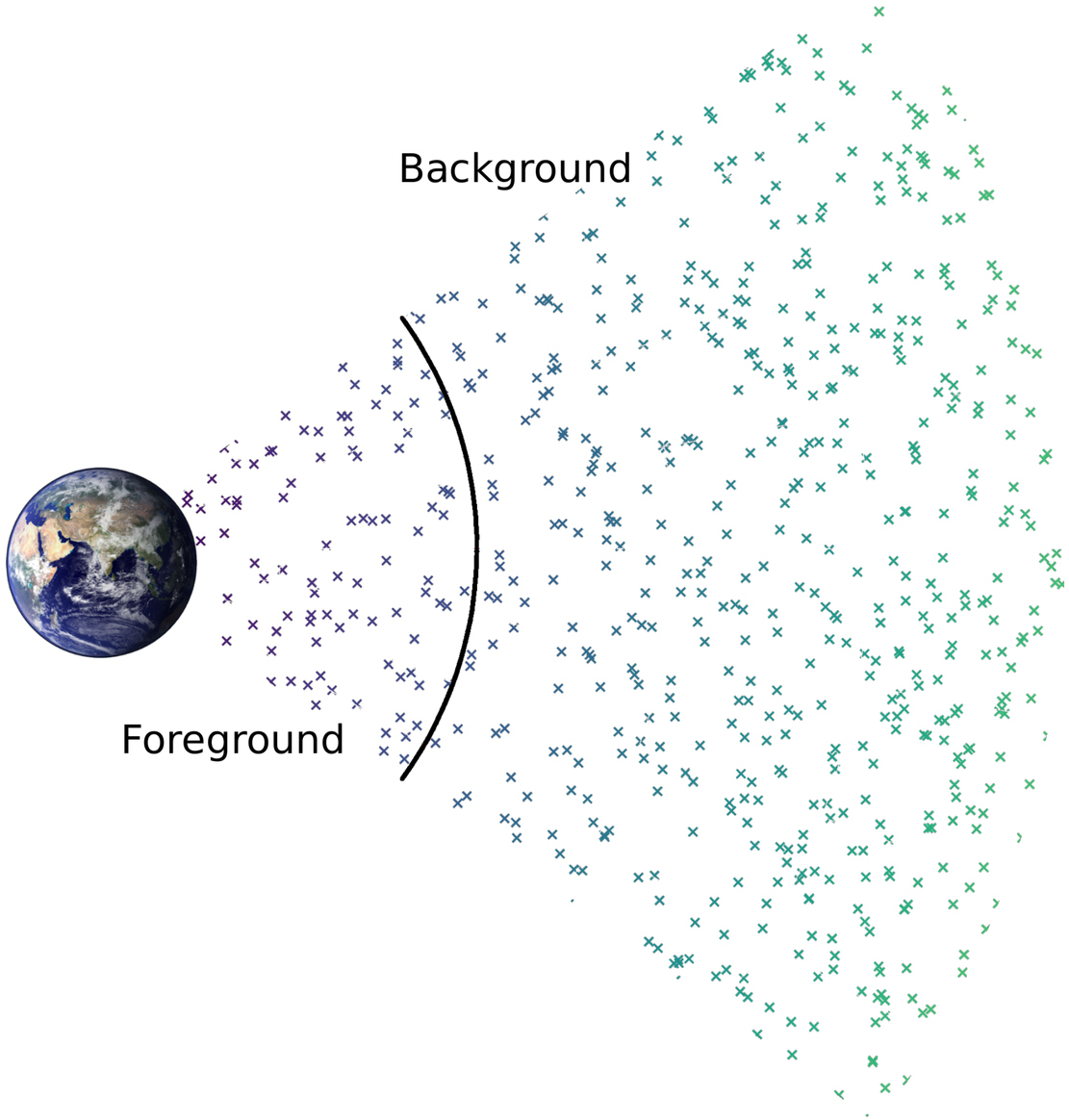

- incoherent, persistent GW signal
- faint/numerous sources
- astrophysical and cosmological
- GW density parameter:

$$\Omega_{\mathrm{GW}}(f) = \frac{1}{\rho_{\mathrm{crit}}} \frac{\mathrm{d}\rho_{\mathrm{GW}}}{\mathrm{d}(\ln f)}$$

Current SGWB constraints

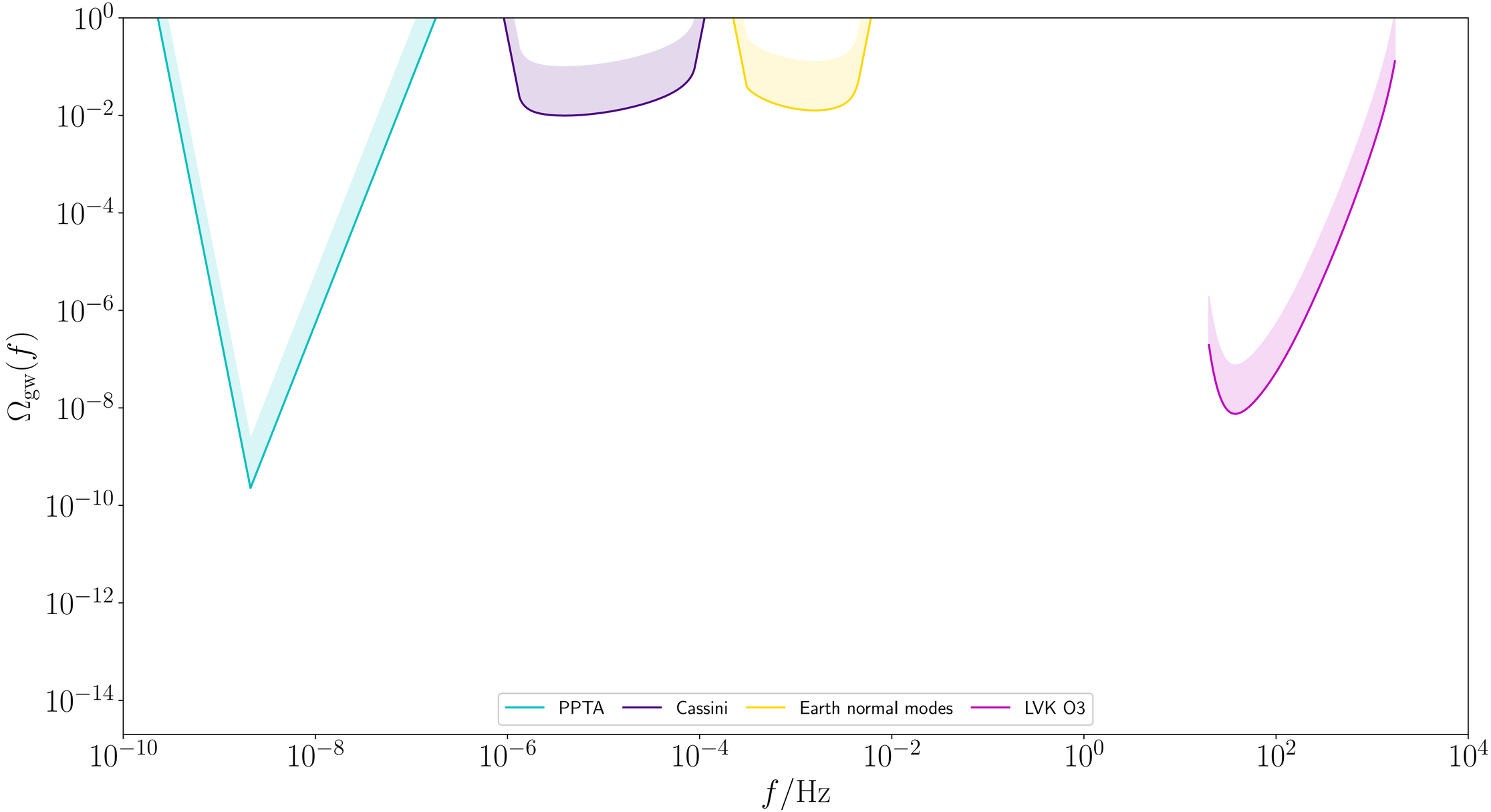

Future SGWB constraints

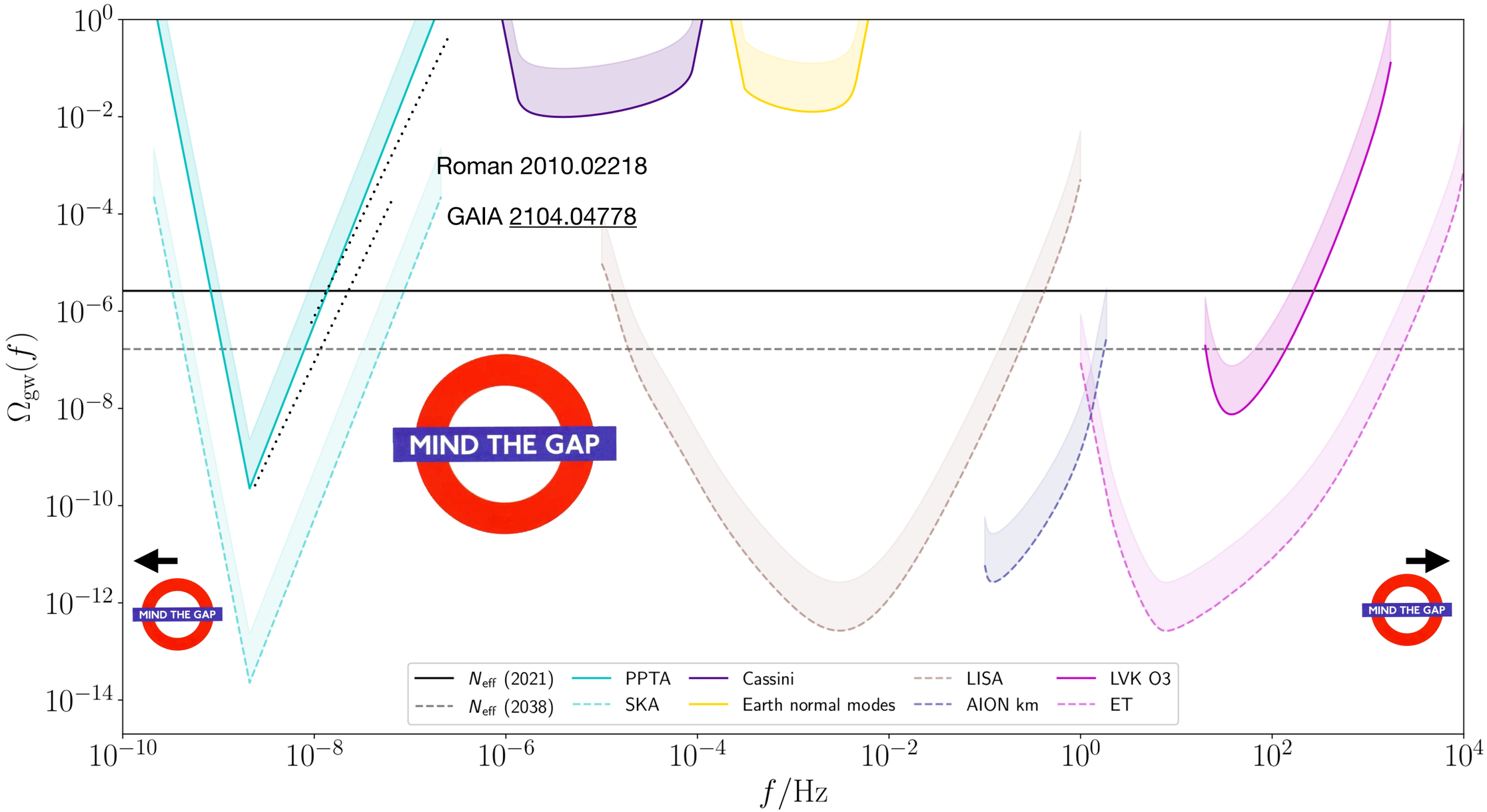

Binary resonance: a brief history

discussed by Misner, Thorne, and Wheeler...

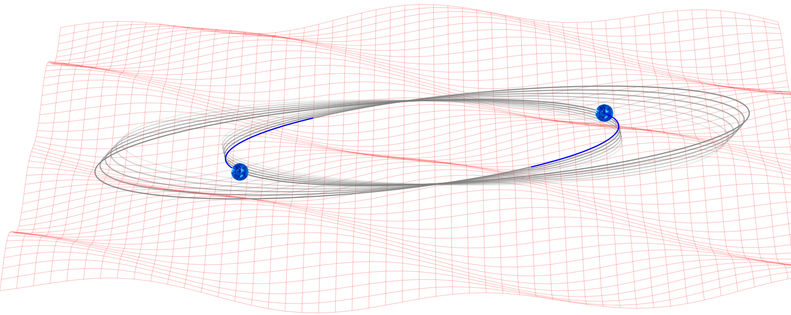

1. The Relative Motions of Two Freely Falling Bodies

As a gravitational wave passes two freely falling bodies, their proper separation oscillates (Figure 37.3). This produces corresponding oscillations in the redshift and round-trip travel times for electromagnetic signals propagating back and forth between the two bodies. Either effect, oscillating redshift or oscillating travel time, could be used in principle to detect the passage of the waves. Examples of such detectors are the Earth-Moon separation, as monitored by laser ranging [Fig. 37.2(a)]; Earth-spacecraft separations as monitored by radio ranging; and the separation between two test masses in an Earth-orbiting laboratory, as monitored by redshift measurements or by laser interferometry. Several features of such detectors are explored in exercises 37.6 and 37.7. As shown in exercise 37.7, such detectors have so low a sensitivity that they are of little experimental interest.

...but that was *50 years ago!*

investigated more recently by Lam Hui *et al*, PRD (2013),
similar ideas used to search for dark matter by Blas *et al*, PRL (2017)

time for a closer look?

Orbital elements

- **period** P**, eccentricity** e:
  size and *shape* of orbit
- **inlination** I**, ascending node** Ω:
  orientation in space
- **pericentre** ω**,**
  mean anomaly at epoch ε:
  radial and angular *phases*

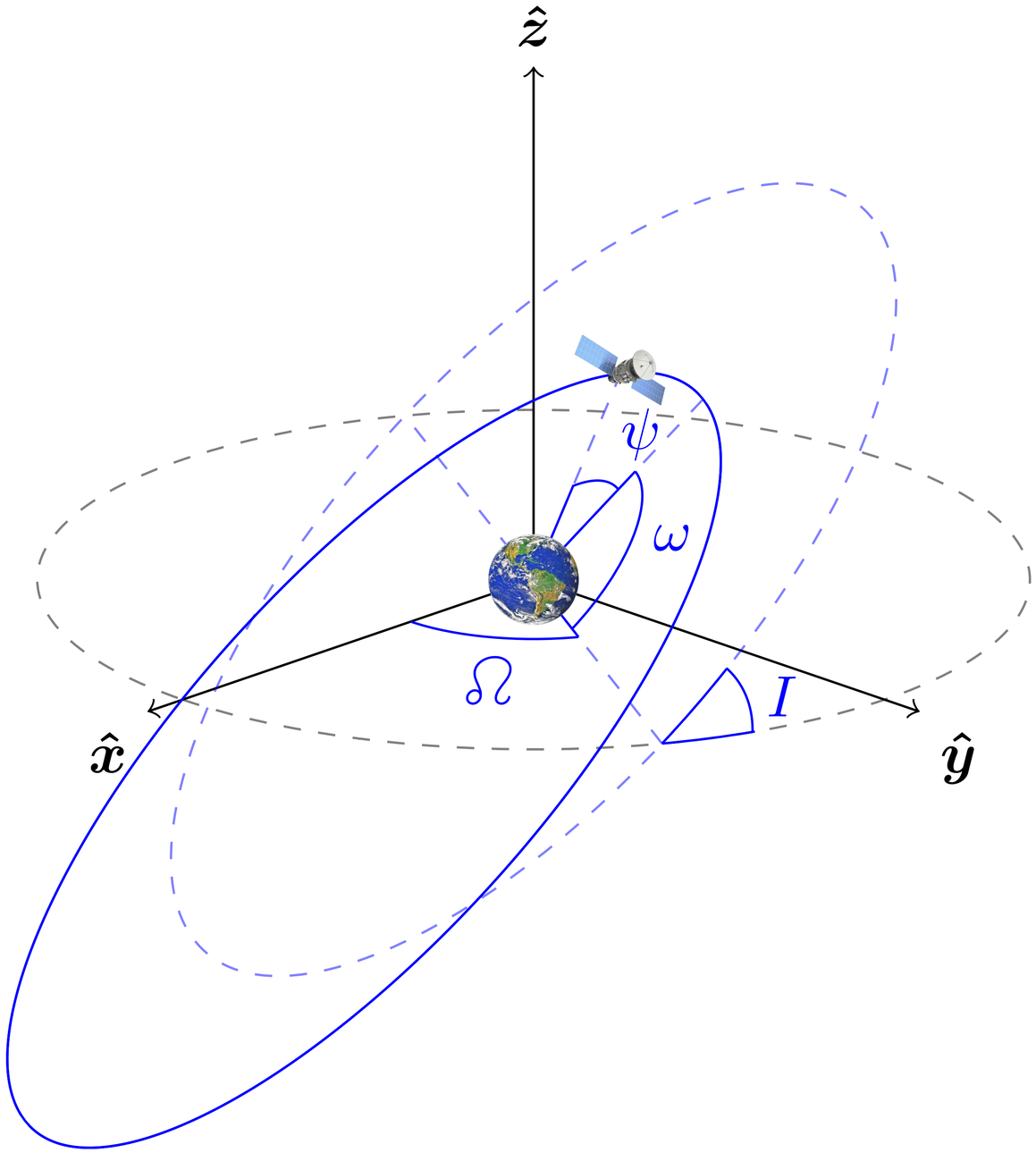

Osculating orbits

$$\delta\ddot{\boldsymbol{r}} = r(\mathcal{F}_r\hat{\boldsymbol{r}} + \mathcal{F}_\theta\hat{\boldsymbol{\theta}} + \mathcal{F}_\ell\hat{\boldsymbol{\ell}}),$$

EoM is instead

$$\ddot{\boldsymbol{r}} + \frac{GM}{r^2}\hat{\boldsymbol{r}} = \delta\ddot{\boldsymbol{r}}.$$

$$\delta\ddot{r}^i = -\delta R^i{}_{0j0} r^j$$

$$\dot{P} = \frac{3P^2\gamma}{2\pi}\left[\frac{e\sin\psi\mathcal{F}_r}{1+e\cos\psi} + \mathcal{F}_\theta\right],$$

$$\dot{e} = \frac{\dot{P}\gamma^2}{3Pe} - \frac{P\gamma^5\mathcal{F}_\theta}{2\pi e(1+e\cos\psi)^2},$$

$$\dot{I} = \frac{P\gamma^3\cos\theta\mathcal{F}_\ell}{2\pi(1+e\cos\psi)^2},$$

$$\dot{\Omega} = \frac{\tan\theta}{\sin I}\dot{I},$$

$$\dot{\omega} = \frac{P\gamma^3}{2\pi e}\left[\frac{(2+e\cos\psi)\sin\psi\mathcal{F}_\theta}{(1+e\cos\psi)^2} - \frac{\cos\psi\mathcal{F}_r}{1+e\cos\psi}\right] - \cos I\dot{\Omega},$$

$$\dot{\varepsilon} = -\frac{P\gamma^4\mathcal{F}_r}{\pi(1+e\cos\psi)^2} - \gamma(\cos I\dot{\Omega} + \dot{\omega}),$$

From Langevin to FP

$$\dot{X}_i(\boldsymbol{X}, t) = V_i(\boldsymbol{X}) + \Gamma_i(\boldsymbol{X}, t),$$

$$\frac{\partial W}{\partial t} = -\partial_i (D_i^{(1)} W) + \partial_i \partial_j (D_{ij}^{(2)} W),$$

with $\partial_i \equiv \partial / \partial X_i$.

$$D_i^{(1)} = V_i + \lim_{\tau \to 0} \frac{1}{\tau} \int_t^{t+\tau} \mathrm{d}t' \int_t^{t'} \mathrm{d}t'' \, \langle \Gamma_j(\boldsymbol{x}, t'') \partial_j \Gamma_i(\boldsymbol{x}, t') \rangle \, .$$

$$D_{ij}^{(2)} = \lim_{\tau \to 0} \frac{1}{2\tau} \int_t^{t+\tau} \mathrm{d}t' \int_t^{t+\tau} \mathrm{d}t'' \, \langle \Gamma_i(\boldsymbol{x}, t') \Gamma_j(\boldsymbol{x}, t'') \rangle \, .$$

Our new approach

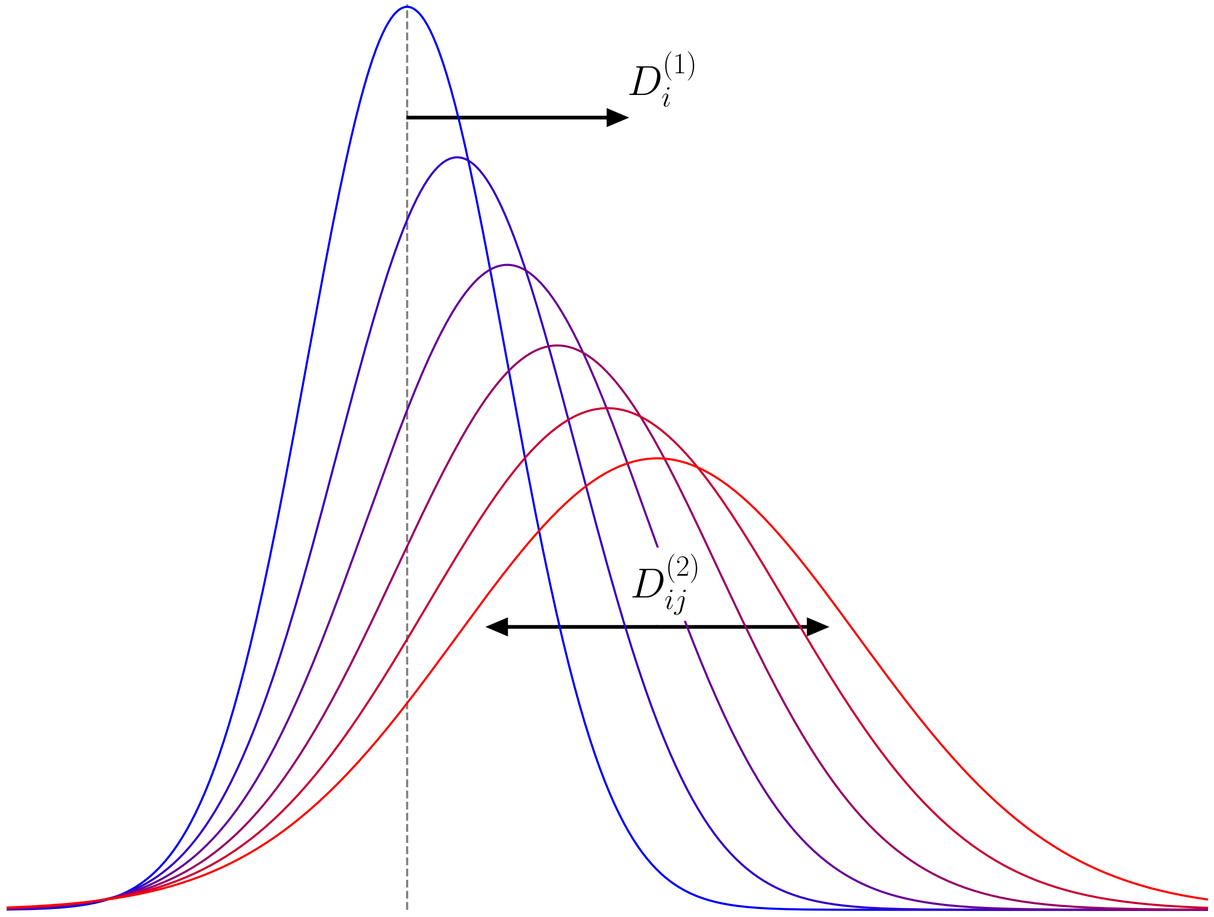

- track distribution function $W(\boldsymbol{X}, t)$ of orbital elements $\boldsymbol{X} = (P, e, I, \Omega, \omega, \varepsilon)$
- evolves through *Fokker-Planck eqn.*

$$\frac{\partial W}{\partial t} = -\frac{\partial}{\partial X_i}\left(D_i^{(1)} W\right) + \frac{\partial}{\partial X_i}\frac{\partial}{\partial X_j}\left(D_{ij}^{(2)} W\right)$$

- *drift* and *diffusion* coefficients

$$D_i^{(1)}(\boldsymbol{X}) = V_i(\boldsymbol{X}) + \sum_{n=1}^{\infty} \mathcal{A}_{n,i}(\boldsymbol{X}) \Omega_{\rm gw}(n/P)$$

$$D_{ij}^{(2)}(\boldsymbol{X}) = \sum_{n=1}^{\infty} \mathcal{B}_{n,ij}(\boldsymbol{X}) \Omega_{\rm gw}(n/P)$$

Two binary probes

timing of binary pulsars

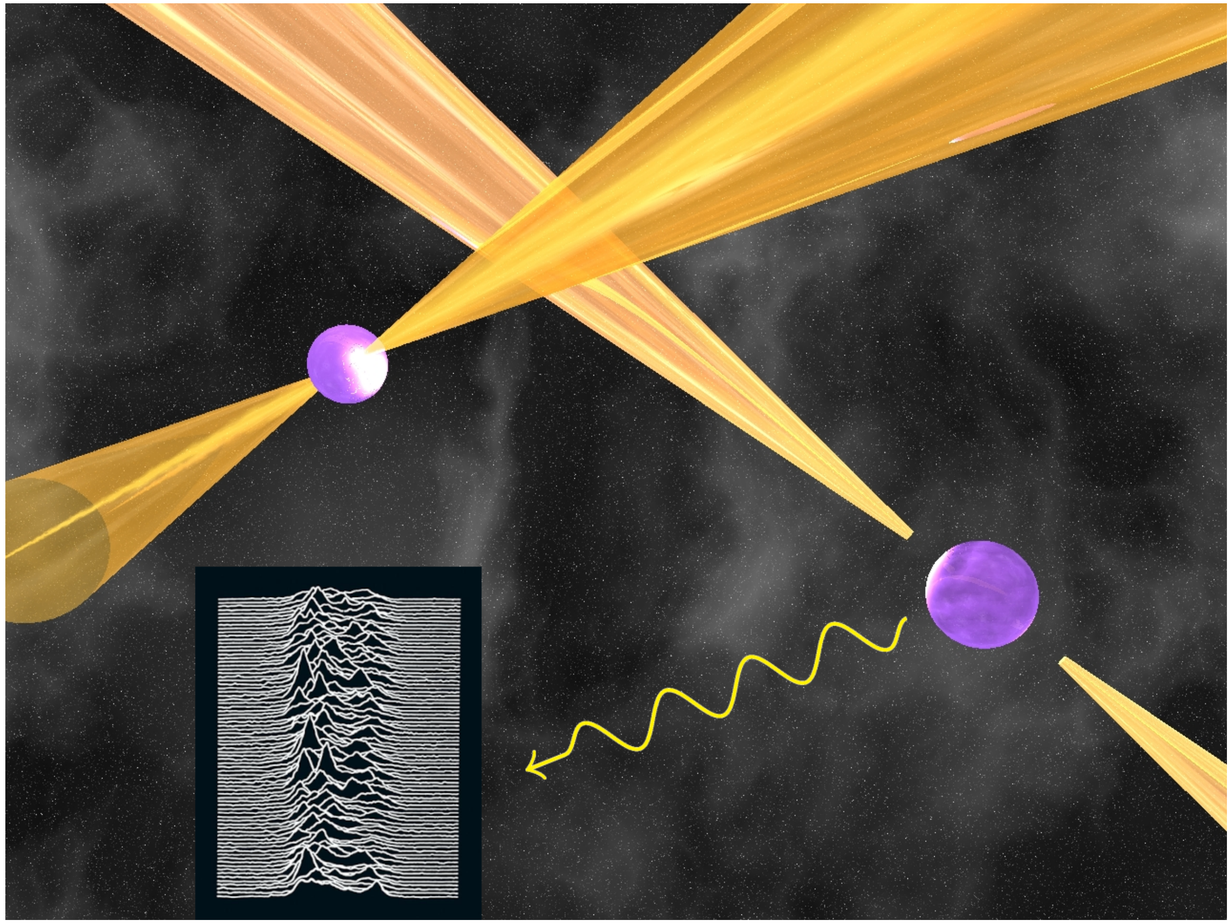

(pulsar animation credit: Michael Kramer)

lunar and satellite laser ranging

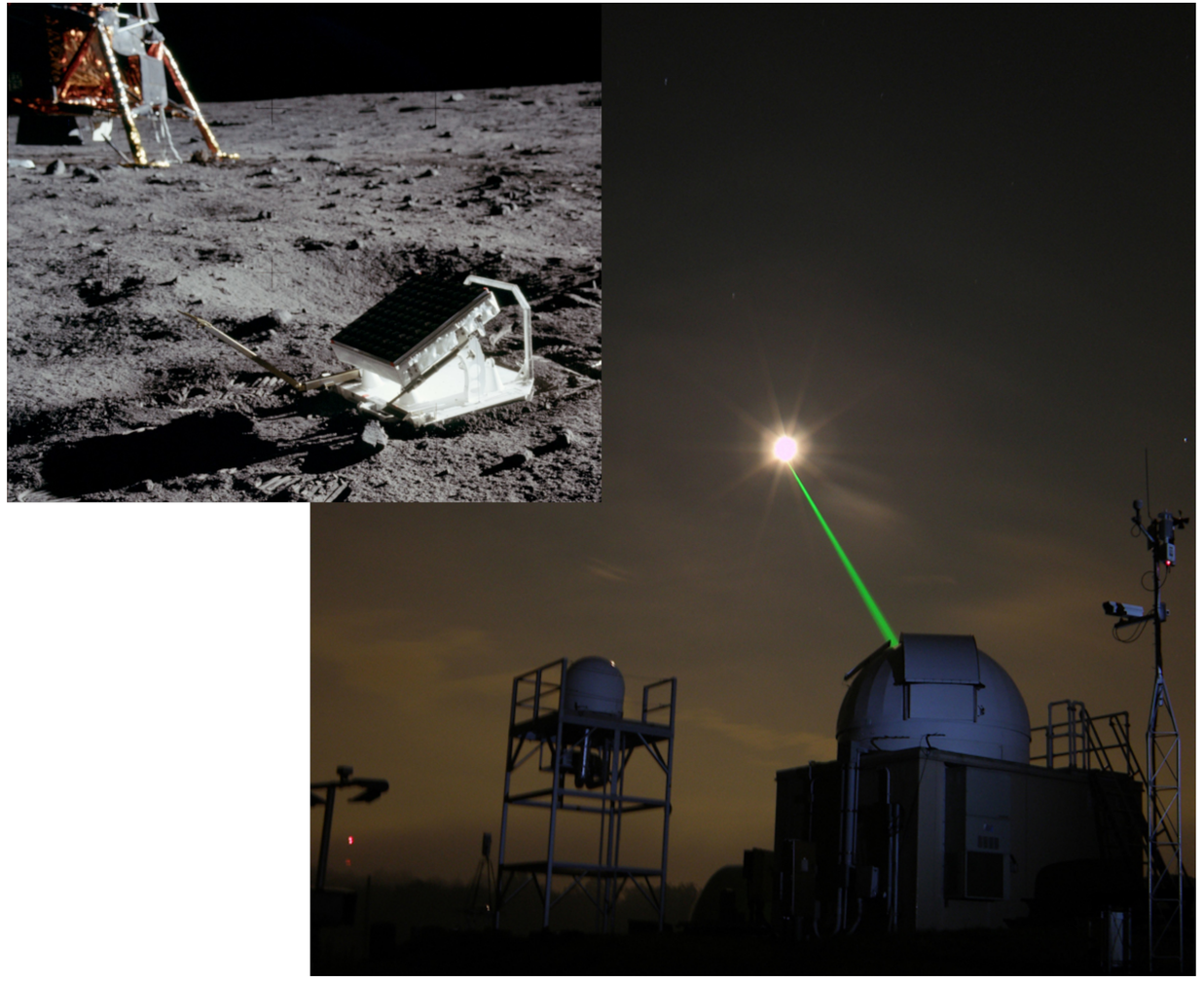

(image credit: NASA)

Our forecast constraints

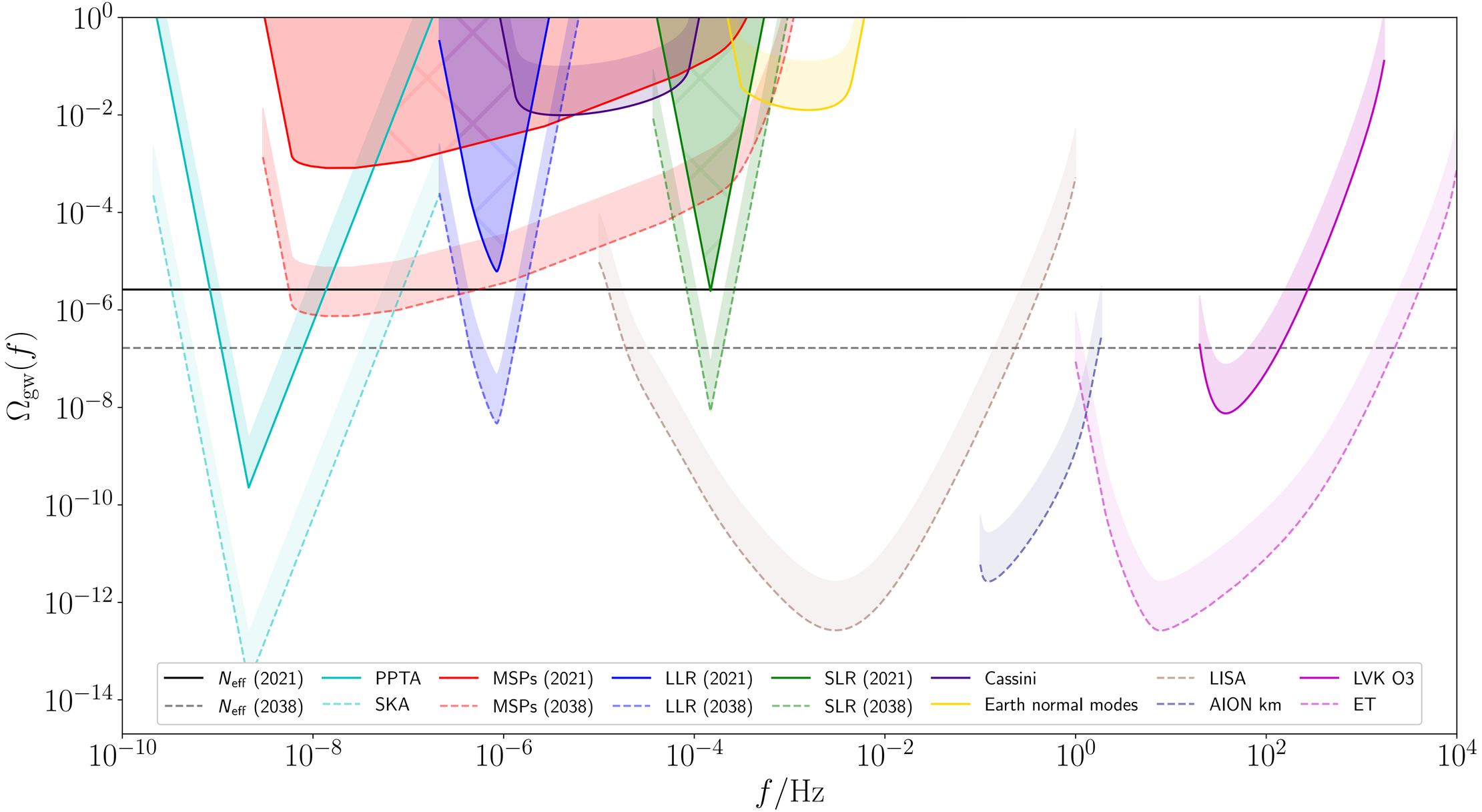

Signals in the μHz band

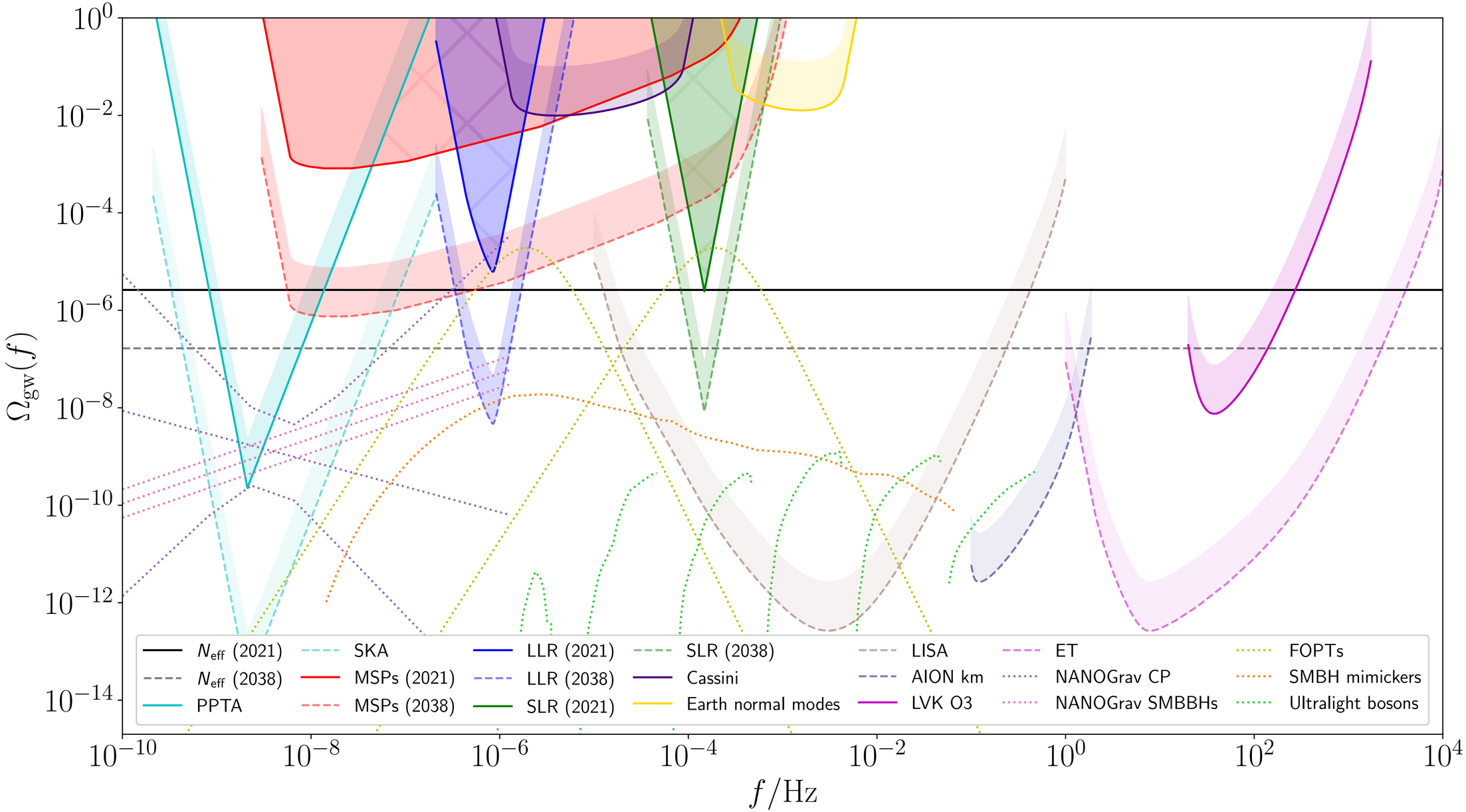

An example signal: cosmological phase transitions

- key prediction of many particle physics models
- four parameters:
  - temperature T_*
  - strength α
  - rate β/H_*
  - bubble-wall velocity v_w
- peak frequency

$$f_* \approx 19\,\mu\text{Hz} \times \frac{T_*}{100\,\text{GeV}} \frac{\beta/H_*}{v_w}$$

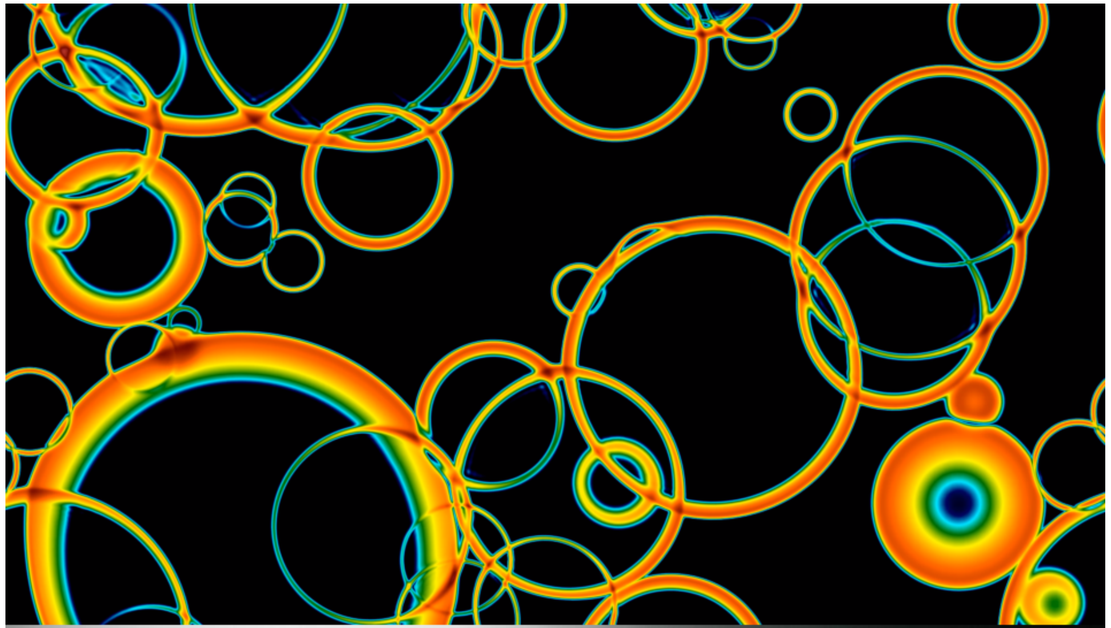

Phase transition constraints

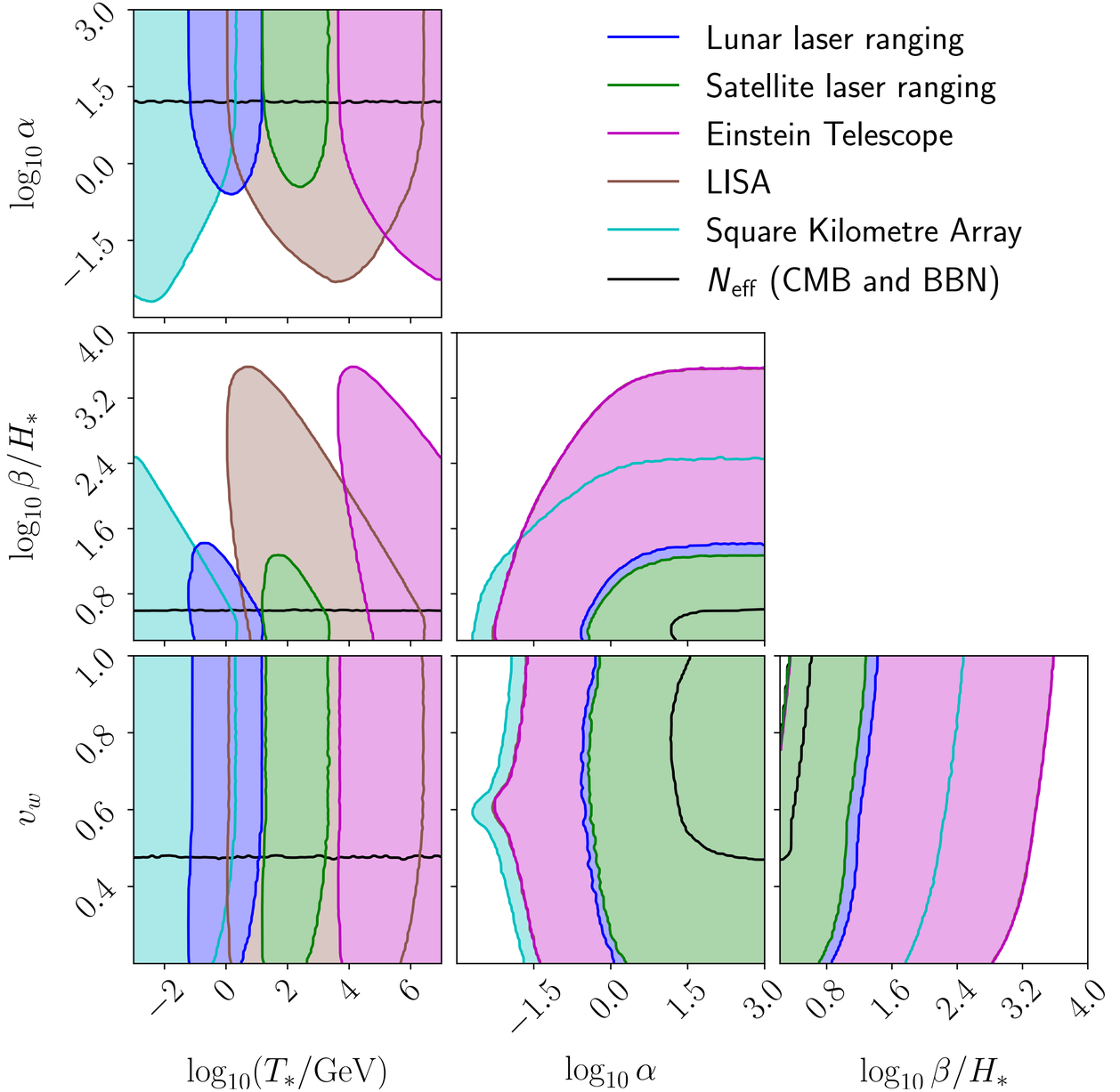

Summary and outlook

- binary resonance can probe a unique GW frequency band
- we have developed a powerful new formalism
- unique constraints on phase transitions (and more)
- plenty more work to do! more signals, more systems, plus running on real data